Studies on Optical Consistency of White LEDs Affected by Phosphor Thickness and Concentration Using Optical Simulation

Zong-Yuan Liu, Sheng Liu, *Senior Member, IEEE,* Kai Wang, and Xiao-Bing Luo, *Member, IEEE*

***Abstract*—Effects of variations of yttrium aluminum garnet:Ce phosphor thickness and concentration on optical consistency of produced white light-emitting diodes (LEDs) including the consistency of brightness and light colors were studied by optical simulation. Five packaging methods with different phosphor locations were compared. Optical models of LED chip and the phosphor were presented and a Monte Carlo ray-tracing simulation procedure was developed. Both color binning and brightness level were used to sort the simulated LEDs to evaluate their optical consistency. Results revealed that the optical consistency of white LEDs strongly depends on how the phosphor thickness and the concentration vary. To obtain desired color binning, conformal phosphor coating is not a favorable packaging method due to its low brightness level and poor brightness consistency by large shifts of the brightness level as the phosphor thickness and concentration varying. Planar remoter phosphor improves the brightness level and its consistency, but realization of high color consistency becomes more difficult due to its smaller variation ranges of the phosphor thickness and concentration. Hemispherical remoter phosphor can fulfill the requirements of both high color consistency and high brightness consistency due to its capability of larger variation ranges of the phosphor thickness and concentration. By applying this method with thick phosphor thickness or high phosphor concentration, this method can be a promising packaging method for the low cost production.**

***Index Terms*—Concentration, light extraction, light-emitting diodes (LEDs), optical consistency, packaging, phosphor, thickness.**

I. Introduction

As an attractive illumination source, white light-emitting diodes (LEDs) have developed rapidly in recent years [1]–[3]. In 1996, a method that applied blue LED chip with yttrium aluminum garnet (YAG):Ce phosphor to generate white light was discovered and first enabled white LED to be commercially available [4]. In 2007, reported luminous efficiency of phosphor-converted LEDs has increased to be more than 100 lm/W for a driving current of 350 mA [1]. The advancements of white LED performance are promoting the applications of white LEDs in areas such as large size flat panel backlighting, street lighting, vehicle forward lamp, museum illumination and residential illumination [5]–[7].

To accelerate the penetration of white LEDs into illumination market, it is critical to reduce the LED cost [8]. The optical consistency, which is named as the ability to control the variation of optical performance of produced LEDs such as luminous efficiency, correlated color temperature (CCT) and color rendering index in desired ranges, is believed to be important for the reduction of the cost. Poor optical consistency means an increase of sale price, since the material cost loss for those LED products with their performance out of requirements of purchasers should be counted in the sale price.

In the studies of the optical consistency of phosphor-converted white LEDs, phosphor thickness and concentration are two important factors. This is because that the phosphor thickness and concentration varies frequently in the manufacturing and, therefore, can directly affect the luminous efficiency and the light color. In most LED packaging processes, phosphor layer is fabricated by a mixture of YAG:Ce phosphor powder and silicone. The mixture is then dispensed around LED chip by dispensing equipment. Since the viscosity of the mixture varies with the pressure, temperature, and time, slight deviations of equipment parameters will affect the flow of the mixture and change its geometry. This change causes variations of the phosphor thickness across the chip. Phosphor concentration also varies because of the slow deposition of the phosphor powder in the mixture before and during curing.

Several innovative techniques such as evaporating solvent [9], electrophoretic deposition [10], Lumiramic plate [11] and wafer-level spin-coating [12] are proposed to maintain the variations of the phosphor thickness and concentration to be in acceptable ranges. These methods fabricate a thinner phosphor layer with uniform thickness by stacking phosphor particles closely. The issue is that the extremely high phosphor con-

Manuscript received February 14, 2009; revised May 18, 2009, September 17, 2009, and December 16, 2009. Date of publication August 16, 2010; date of current version December 22, 2010. This work was supported by the National Natural Science Foundation of China, under Project 50835005. Recommended for publication by Associate Editor M. Arik upon evaluation of reviewers' comments.

Z.-Y. Liu and S. Liu are with the School of Mechanical Science and Engineering, Huazhong University of Science and Technology, Wuhan 430074, China, and also with the Wuhan National Laboratory for Optoelectronics, Wuhan 430074, China (e-mail: liuzy85@gmail.com; victor_liu63@126.com).

K. Wang is with School of Optoelectronics Science and Engineering, Huazhong University of Science and Technology, Wuhan 430074, China, and also with the Wuhan National Laboratory for Optoelectronics, Wuhan 430074, China (e-mail: kaiwang83@gmail.com).

X.-B. Luo is with School of Energy and Power Engineering, Huazhong University of Science and Technology, Wuhan 430074, China, and also with the Wuhan National Laboratory for Optoelectronics, Wuhan 430074, China (e-mail: luoxb@mail.hust.edu.cn).

Color versions of one or more of the figures in this paper are available online at http://ieeexplore.ieee.org.

Digital Object Identifier 10.1109/TCAPT.2010.2044576

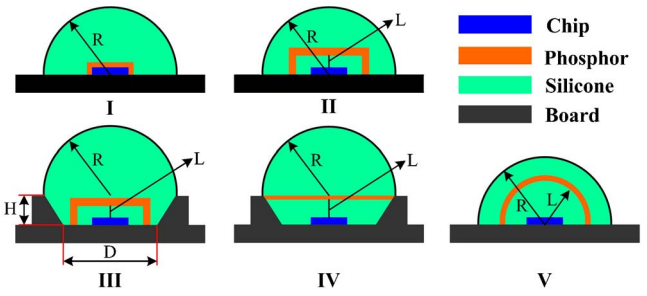

Fig. 1. Schematic illustration of the five packaging methods for the simulation. L represents the phosphor location. In Methods II, III, and IV, L is the gap between phosphor and chip. In Method V, *L* is the length of phosphor. Radius (*R*) is 4 mm. The baseline diameter (*D*) of reflector is 3 mm and the height (*H*) is 2 mm.

TABLE I

PHOSPHOR LOCATIONS IN FIVE PACKAGING METHODS

Methods	I	II	III	IV	V
Location (mm)	0	0.05	0.05	1.8	2

centration in these methods causes the optical performance to be more sensitive to slight variation of the phosphor thickness.

There are other packaging methods that do not involve directly coating the phosphor on the chip such as planar remoter phosphor [13], [14], scattered photon extraction (SPE) [15], [16], hemispherical remoter phosphor [17], [18]. These techniques, except SPE, all suffer from lack of standard processes to fabricate high quality phosphor layer. In the packaging method with planar remoter phosphor, mismatch of surface tensions between the silicone and the phosphor layer can generate nonuniform phosphor thickness. For the hemispherical remoter phosphor, the slow deposition of phosphor particles in the mixture during curing is serious.

Therefore, no matter how the phosphor is fabricated in white LED production, the issue of optical consistency caused by variations of phosphor thickness and concentration is inevitable and needs to be studied. Sommer *et al.* [19] have found that changing the phosphor thickness and concentration can affect the spatial color distribution. This paper focuses the study on the consistency of brightness and light color, and simulates five packaging methods with different geometries by Monte Carlo ray-tracing. Two issues are concerned: 1) how the optical performance of these packaging methods is affected by the phosphor thickness and concentration; and 2) which packaging method can improve the optical consistency by its geometry. Definitions of the optical models of white LEDs and the simulation procedure are given in Section II. The simulation results of five packaging methods are compared and discussed in Section III.

II. NUMERICAL MODELS AND ANALYTICAL METHOD

A. Descriptions of Five Packaging Methods

As depicted in Fig. 1, five packaging methods are simulated in this paper. Each packaging element is represented by one color. Methods I, II, and III coat the phosphor with a rectangular shape by a replication of the chip geometry. The difference is that there is a small gap between the phosphor and the chip in Methods II and III, whereas the phosphor is directly dispensed on the chip surface in Method I, which is named as conformal phosphor coating. In Method IV, the phosphor is planar shape but the location is remoter, naming as a planar remoter phosphor. Method V fabricates the phosphor with hemispherical shape by naming it as hemispherical remoter phosphor [17]. The phosphor location of each packaging method is illustrated in Table I.

In Methods III and IV, the cavity in the board is used as a reflector. Surfaces of the board and the reflector are coated with Ag to provide high reflection. Simulation assumes the reflectance of these surfaces to be 95% [13], [14]. Silicone is used to fabricate the hemispherical lens, to fill the reflectors in Methods III and IV, and to fill the gaps between the phopshor and the chip in Methods II and V. In the optical simulation, the refractive index and absorption coefficient of the silicone are set to be 1.5 and 0 mm^{-1}, respectively.

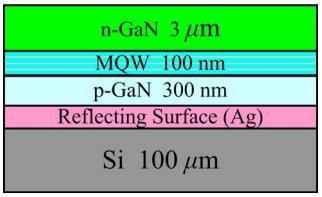

Fig. 2. Schematic illustration of vertical injection chip model.

TABLE II

OPTICAL PROPERTIES OF CHIP

Item	n-GaN	MQW	p-GaN
Refractive Index	2.42	2.54	2.45
Absorption Coefficient (mm^{-1})	5	8	5

B. Chip Model

The simulated LED chip model is shown in Fig. 2. This chip is one 1 mm × 1 mm vertical injection chip with silicon substrate. The bottom surface of p-GaN is deposited with Ag to provide high reflection. Simulation assumes the reflectance of this surface to be 92% specular reflection and 4% diffuse scattering [20]. Blue light is isotropically emitted from multiple quantum-well (MQW) layer with uniform distribution. Considering that the area of top and down surfaces of MQW layer is much larger than that of its side surfaces, model sets these two surfaces as the light sources and ignores light emitted from the side surfaces.

The optical parameters of chip materials are illustrated in Table II [21]. Light extraction efficiency of chip is calculated to verify the feasibility of the chip model. Computational result of the light extraction efficiency is 14.32%. Considering that internal quantum efficiency of an actual chip is around 70%, the external quantum efficiency, which is a multiplication of the light extraction efficiency and the internal quantum efficiency, will be around 10.02%. This value is reasonable according to published results [22].

C. Phosphor Model

In the five packaging methods, the phosphor layer is a mixture of the phosphor powder and the silicone. Since refractive index of the phosphor powder is larger than that of the silicone, a photon entering the mixture will be scattered many times during its propagation. For each scattering, this photon is absorbed by the phosphor particle and subsequently scattered to other directions. The simulation treats the mixture as an independent flourescent material with independent refractive index, bulk absorption and emission, and Mie scattering properties. Refractive index of the mixture (n_{mix}) is obtained by the refractive index mixture rules [23]

$$n_{\text{mix}} = \phi_{\text{phos}} n_{\text{phos}} + \phi_{\text{sil}} n_{\text{sil}} \tag{1}$$

where ϕ_{phos} and ϕ_{sil} are volume fractions of the phosphor powder and the silicone in the mixture, respectively; n_{phos} and n_{sil} are refractive indices of the phosphor powder and the silicone, respectively. Simulation assumes n_{phos} and n_{sil} to be 1.85 and 1.5.

ϕ_{phos} has a relationship with the phosphor concentration c (g/cm^3) as

$$c = \rho \phi_{\text{phos}} = \tfrac{4}{3}\pi r^3 \sigma \rho \tag{2}$$

where ρ is density of the phosphor, r is mean radius of the phosphor particles, and σ is the particle number in unit mixture. ρ and r are assumed to be 4.5 g/cm^3 and 2.2 μm in this simulation.

According to the excitation and emission spectra of YAG:Ce phosphor, YAG:Ce phosphor shows high absorption for the blue light spectra and weak absorption for the converted-yellow light spectra around 500 nm. At the first step, simulation calculates absorption and scattering parameters of the mixture for the blue light and the converted-yellow light separately by Mie theory [24]

$$\mu_\alpha(\lambda) = \sigma C_\alpha(\lambda), \qquad \mu_s(\lambda) = \sigma C_s(\lambda) \tag{3}$$

$$g(\lambda) = 2\pi \int p(\theta, r) \cos\theta \mathrm{d}\theta \tag{4}$$

where μ_α, μ_s, and g are absorption coefficient, scattering coefficient, and anisotropy factor, respectively; C_α and C_s are absorption and scattering cross-sections, respectively; $p(\theta,r)$ is the phase function, θ is the scattering angle, and λ is the light wavelength. Calculation of C_α, C_s, and $p(\theta,r)$ requires knowing of imaginary refractive indices of the phosphor, which are assumed to be 7.24×10^{-4} for blue light and 9.47×10^{-6} for converted-yellow light, respectively.

Since the actual phosphor particle size is nonspherical, the second step is modifying the Mie theoretical results of the first step by the experimental data [25], [26]. Fitting factors k_α and k_s are used to obtain modified parameters

$$\mu'_a = k_\alpha \mu_\alpha, \qquad \mu'_s = k_s \mu_s, \qquad g' = g/k_s \tag{5}$$

where μ'_α, μ'_s, and g' are modified absorption coefficient, scattering coefficient, and anisotropy factor, respectively. k_α and k_s for the blue light are set to be 1.5 and 1.01, respectively. For the converted-yellow light, Mie theory shows good approximation for the actual light scattering. k_α and k_s are therefore set to be 1.2 and 1, respectively.

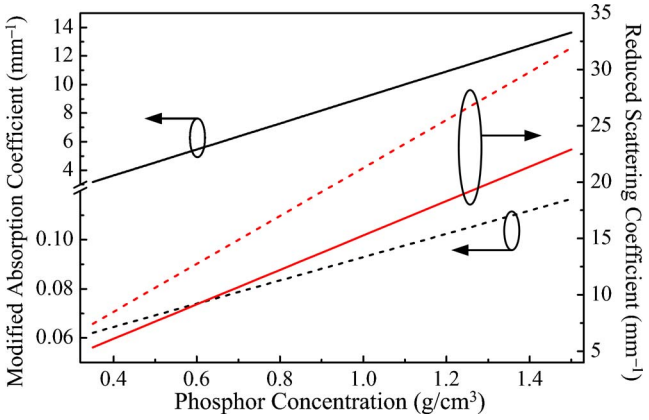

Fig. 3. Modified absorption coefficient (μ'_α) and reduced scattering coefficient (ξ_s) of YAG:Ce phosphor mixture for different phosphor concentrations. The solid lines are μ'_α and ξ_s for the blue light, and dashed lines are μ'_α and ξ_α for the converted-yellow light.

Finally, according to Lambert-Beer law, reduced scattering coefficient ξ_s is introduced to treat the simulated phosphor mixture as isotropic scattering

$$I(t) = I_0 \exp\{-[\mu'_\alpha + \mu'_s(1-g')]t\} = I_0 \exp[-(\mu'_\alpha + \xi_s)t] \tag{6}$$

where I_0 is the optical power of incident light, $I(t)$ is the optical power of transmitted light, and t is the phosphor thickness. The calculated μ'_α and ξ_s for different phosphor concentrations are shown in Fig. 3.

To determine directions of the scattered light by the phosphor particles in the ray-tracing, simulation uses Henyey-Greenstein model to calculate the phase function $p(\cos\theta)$

$$p(\cos\theta) = \frac{1-g^2}{2(1+g^2-2g\cos\theta)^{3/2}}. \tag{7}$$

Power conversion efficiency of the phosphor is obtained by multiplying the Stokes efficiency (quantum deficit) with the quantum efficiency [7], [27], [28]. Stokes efficiency is the quantum ratio of average emission wavelengths of the chip and the phosphor. In this simulation, the average wavelengths of the blue light and the converted-yellow light are assumed to be 459 nm and 568 nm, respectively. The quantum efficiency is normally larger than 90%, and can be higher than 95% [29]. Therefore, the power conversion efficiency will be larger than 76.77% and this simulation sets it to be 77%, which is reasonable when comparing with the experimental results [26].

D. Analytical Method

The simulation procedure is illustrated in Fig. 4 by using Monte Carlo ray-tracing. Total number of the traced rays is 2 000 000, in which 1 000 000 rays are the blue light and the other 1 000 000 rays are the converted-yellow light. During the ray-tracing, energy of light rays is calculated by optical power in watts. The threshold of light rays is 10^{-4}. To simplify Monte Carlo ray-tracing and shorten the simulation time, simulation assumes the optical parameters above to be invariant for the whole spectra of the blue light and the converted-yellow

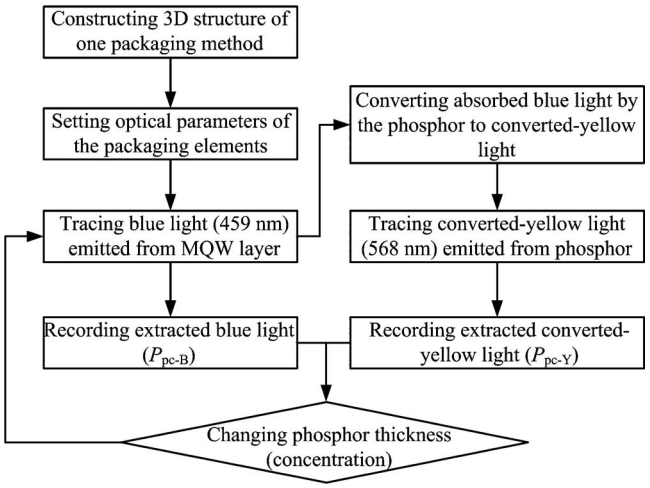

Fig. 4. Flow diagram of the optical simulation procedure.

TABLE III
VARIATIONS OF PHOSPHOR THICKNESS AND CONCENTRATION

Case	1	2	3	4	5
Phosphor Thickness (μm)	60	100	140	40–200	
Phosphor Concentration (g/cm^3)	0.4–1.4			0.6	1

light. Therefore, light rays with single wavelength are used to represent the blue light and the converted-yellow light, which are set to be 459 nm and 568 nm, respectively. This simplification has been proven to be effective for the optical simulation of LED and adopted by many studies to predict LED performance [13], [14], [19], [30]–[32].

For each packaging method, five variation cases of the phosphor thickness and the concentration are simulated as shown in Table III. In each case, only the phosphor thickness or the concentration changes. From one case to another case, both the phosphor thickness and the concentration change. As shown in Fig. 4, each packaging method is repeatedly ray traced by the varied phosphor thickness or concentration until the variation range of one case has been completely covered.

The finally obtained results are extracted optical power of the blue light (P_{pc-B}) and the converted-yellow light (P_{pc-Y}). Then, luminous efficiency (η) and color mixing fraction (f) are used to describe the brightness and the light color of white LEDs

$$\eta = 683\ \text{lm/W} \times \frac{P_{pc-B}V_{pc-B} + P_{pc-Y}V_{pc-Y}}{P_{elec}} \tag{8}$$

$$f = P_{pc-Y}/(P_{pc-B} + P_{pc-Y}) \tag{9}$$

where P_{elec} is the consumed electrical power, and V_{pc-B} and V_{pc-Y} are eye sensitivity coefficients for blue light spectra and converted-yellow light spectra, respectively. P_{elec} is 1 W in this paper and the simulation assumes the electrical power to be fully converted to the optical power. V_{pc-B} and V_{pc-Y} are calculated by the measured spectra of one blue LED and one YAG:Ce phosphor and determined to be 0.073 and 0.703, respectively.

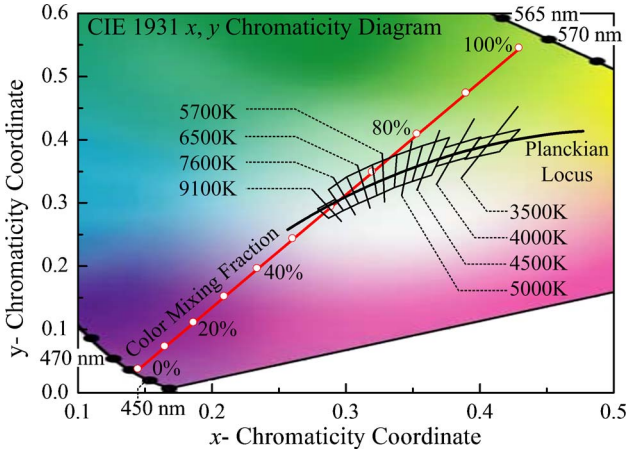

Fig. 5. Variation of color mixing fraction in the x, y chromaticity diagram. The quadrangular color binning is given by the ANSI Standard C78. 377-2008 and the chromaticity specification of Cree Inc.

Fig. 5 shows the relationship of the color mixing fraction and the light color [20]. Color coordinates at the color mixing fractions of 0% and 100% are color points of the blue light and the converted-yellow light, respectively. It can be found that the line of the color mixing fraction intersects with four quadrangles of the color binning in terms of 5700 K, 6500 K, 7600 K, and 9100 K. This paper will discuss the simulated LEDs with their light color in the range of the four quadrangles to study the differences of their optical consistency.

III. RESULTS AND DISCUSSION

The simulation results are shown in Figs. 6 and 7. It can be found that the brightness and the light color of the five packaging methods change variously as the phosphor thickness or concentration varies. This means that their optical consistency is also different. Generally, when the phosphor thickness or concentration varies in the same range, the luminous efficiency and the color mixing fration of Method IV changes slower than those of other methods. The luminous efficiency of Methods I and V increases more rapidly than that of other methods as the phosphor thickness or concentration increases, and the luminous efficiency of Method V is higher than that of Method I. The color mixing fractions of Methods I and V are always close, meaning similar variations of their light color. The luminous efficiency and color mixing fractions of Methods II and III vary similarly and their variations are moderate among the five packaging methods.

An explanation is given in below to clarify the differences of the performance variation of the five packaging methods. For Method I, since the phosphor is directly coated on the chip surface, both the back scattered blue light and the converted-yellow light are strongly absorbed by the chip. Therefore, the chip absorption of Method I is the highest among the five methods. But more blue light can be extracted from the chip because the material coated on the chip is phosphor, refractive index of which is higher than that of silicone in other methods. For Methods II and III, the chip absorption for the back scattered light is reduced because of the small

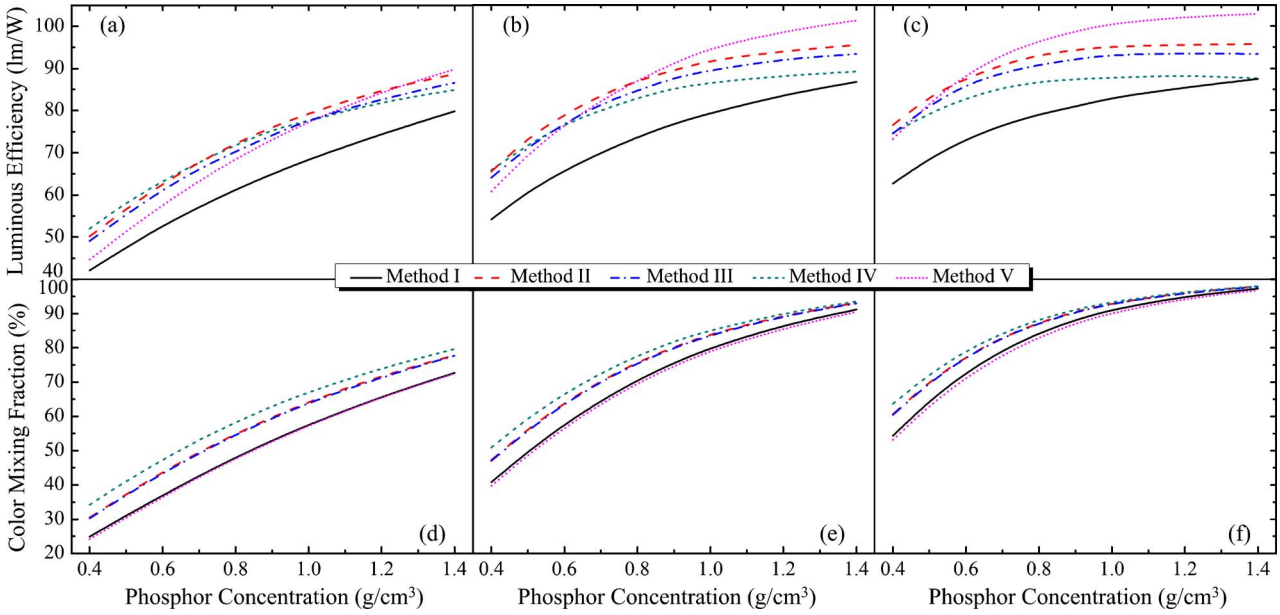

Fig. 6. Dependences of luminous efficiency and color mixing fractions of the five packaging methods on the phosphor concentration for (a) and (d) Case 1, (b) and (e) Case 2, and (c) and (f) Case 3.

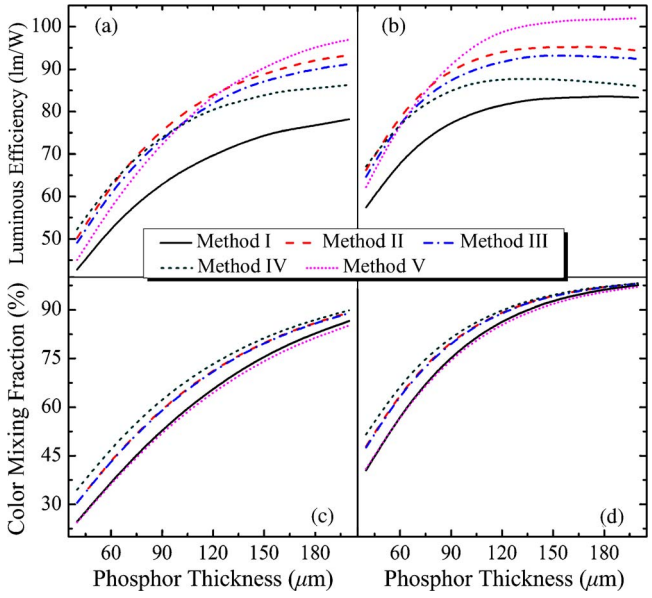

Fig. 7. Dependences of luminous efficiency and color mixing fractions of the five packaging methods on the phosphor thickness for (a) and (c) Case 4, and (b) and (d) Case 5.

gap between the phosphor and the chip. For Method III, light passing through the phosphor may be reflected on the reflector and losses a little energy. In Method IV, the chip absorption for the back scattered light is less than that of Methods II and III but the reflection loss is more serious, because the remoter phosphor of Method IV causes most of the back scattered light to be multiple reflected on the reflector, size of which is much larger than that of the chip. This multiple reflections also enhance the conversion of the blue light by the phosphor. Comparing with Method IV, the hemispherical remoter phosphor of Method V is capable of high extraction of the blue light and the converted-yellow light simultaneously. First, the chip is located at the center of the phosphor, therefore, the blue light can more easily pass through the phosphor and reduce the back scattered blue light. Second, the reflection area of Method V is smaller than that of Method IV, and the multiple reflections of Method V are less than those of Method IV. This means that less reflection loss occurs for Method V. Finally, when the phosphor thickness or concentration increases, the phosphor scattering is enhanced and these light losses of the five packaging methods will be changed differently. Higher light losses mean smaller variations of the luminous efficiency and the color mixing fraction, and thus contribute to the performance differences of the five packaging methods.

Comparing the variations of the luminous efficiency and the color mixing fraction of each packaging method from Case 1 to Case 5, another important finding is that the performance variation of one packaging method is different when both the phosphor thickness and the concentration change. Generally, the luminous efficiency and the color mixing fraction for a packaging method with thicker phosphor thickness and higher phosphor concentration change slower than those with thinner thickness and lower concentration, when the same variation of the phosphor thickness or concentration occurs. This difference can be explained by (6), in which $I(t)$ exponentially depends on the variations of the phosphor thickness and the concentration. As a result, it can be deduced that the performance variation of natural white LEDs is generally smaller than that of cool white LEDs.

The discussion above is from an ideal view that assumes all of the light color of the simulated LEDs to be usable white light. However, from the practical view, the light color of white LEDs should be controlled in standard color binning as shown in Fig. 5. Generally, LED manufacturers prefer using the color binning and the brightness level to sort products. In the following, the simulated LEDs are first sorted by the color

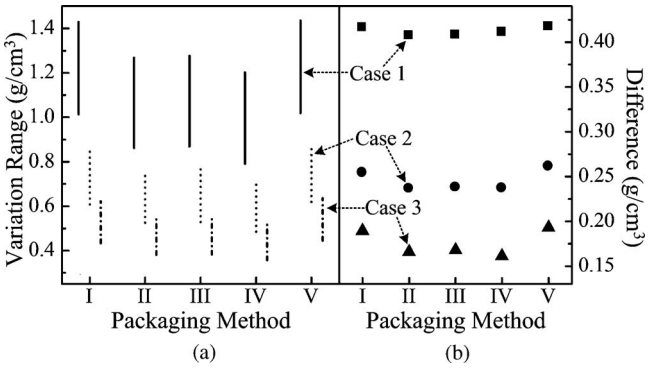

Fig. 8. (a) Variation ranges of the phosphor concentration and (b) phosphor concentration differences of the five packaging methods in Cases 1, 2, and 3 with their light color in the color binning.

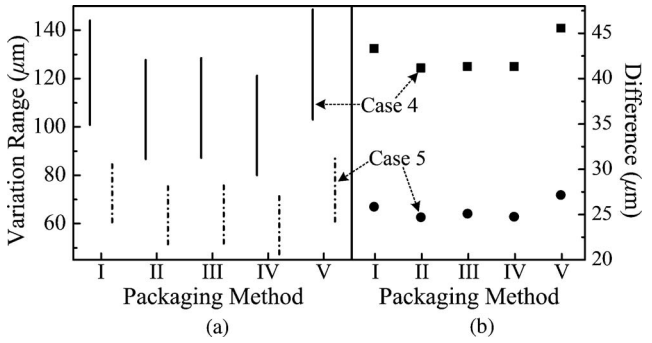

Fig. 9. (a) Variation ranges of the phosphor thickness and (b) phosphor thickness differences of the five packaging methods in Cases 4 and 5 with their light color in the color binning.

binning to investigate their phosphor thickness differences and the concentration differences. Then, the luminous efficiency of the simulated LEDs with their light color keeping in the four-color quadrangles is compared to distinguish their brightness levels.

According to the color binning, the usable ranges of the phosphor concentration and thickness of the five packaging methods are shown in Figs. 8(a) and 9(a). The concentration difference and the thickness difference of these ranges are also given in Figs. 8(b) and 9(b). Generally, the packaging method with larger thickness difference and concentration difference can more easily realize high color consistency. It can be found that the thickness difference and concentration difference of Method V are always larger than those of other methods. The improvement of the color consistency is 19.78% by Method V in Case 3 when comparing with that of Method IV, and 5.19% in Case 4 when comparing with that of Method I. In general, the color consistency of Method I is close to that of Method V, and the color consistency of Methods II, III, and IV is the poorest among the five methods.

From Figs. 8 and 9, it also can be found that the concentration difference and thickness difference are normally larger for the packaging method with thinner phosphor thickness or lower phosphor concentration. This gives the reasons why the conformal phosphor coating is widely adopted in LED packaging, and LED manufacturers without conformal coating equipment prefer using low phosphor concentration.

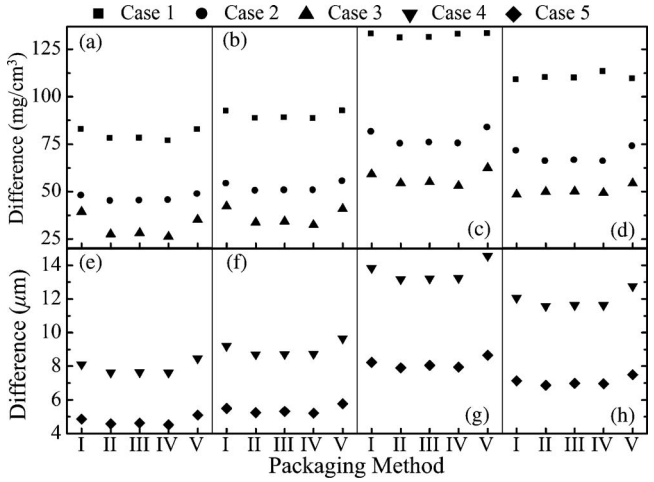

Fig. 10. (a)–(d) Phosphor concentration differences and (e)–(h) phosphor thickness differences of the five packaging methods in the four color quadrangles of the color binning. (a) and (e), (b) and (f), (c) and (g), and (d) and (h) are the differences in color quadrangles of 9100 K, 7600 K, 6500 K, and 5700 K, respectively.

The phosphor concentration difference and the thickness difference in each color quadrangle are further given as shown in Fig. 10. Similar conclusions can also be derived as the above. The color consistency of Method V is better than that of other methods in most cases except in the color quadrangles of 9100 K and 7600 K of Case 3, in which the concentration differences of Method V are smaller than those of Method I.

For the four color quadrangles, the concentration difference and the thickness difference in color quadrangles with higher CCT are normally smaller that those with lower CCT, implying that high color consistency for natural white LEDs can be more easily realized. When the phosphor concentration is too high, high color consistency may be unrealizable for the color quadrangles with higher CCT, since the variation range of the phosphor thickness is too small. For example, in the color quadrangles of 9100 K and 7100 K of Case 5, the thickness difference is only 4–5μm that is equal to the mean size of the phosphor particles, causing precise control of the phosphor thickness to be very difficult.

Fig. 11 shows variation ranges of the luminous efficiency of the five packaging methods with their light color meeting the color binning. It can be found that the brightness level of Method V is the highest among the five methods, and the brightness level of Method I is the lowest. Therefore, the performance/price ratio of Method V can be the highest for the same color binning.

From Fig. 11(a), when both the phosphor thickness and the concentration vary, the luminous ranges of Method I change more obviously than that of other methods. This means that the brightness level of Method I is difficult to be controlled by the phosphor thickness and concentration, causing poor brightness consistency. As shown in Fig. 11(b), the brightness difference of Method I also strongly depends on how the phosphor thickness and the concentration vary. Oppositely, Methods II, III, and V show more stable changes of the luminous ranges and the brightness differences, and the variation of Method V can be the least. The shift of brightness level of

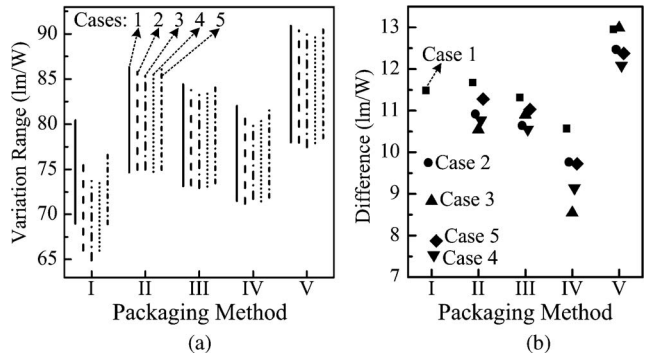

Fig. 11. (a) Variation ranges of the luminous efficiency and (b) brightness differences of the five packaging methods with their light color in the color binning.

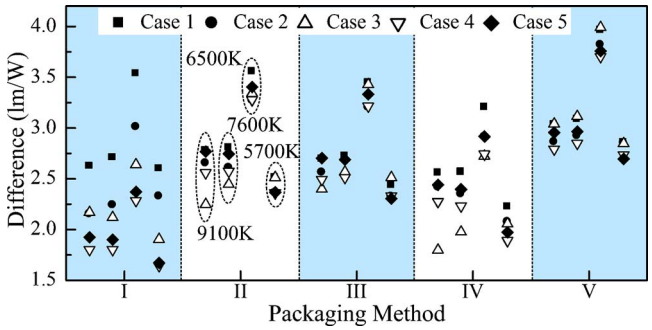

Fig. 12. Brightness differences of the five packaging methods with their light color in each of the four quadrangles of the color binning.

Method IV is better than that of Method I but poorer than that of other methods. Therefore, Methods II, III, and V can more easily realize the same brightness level for the same color binning, showing higher brightness consistency.

The brightness differences of the five packaging methods are small in each color quadrangle as shown in Fig. 12, generally not more than 5 lm/W. The value of the brightness difference of Method V is normally larger than that of other methods. From the discussion above, this is mainly due to its larger variation ranges of the phosphor thickness and the concentration. By controlling the variations of the phosphor thickness and the concentration in smaller ranges, the brightness difference of Method V will be reduced. If applying thicker phosphor thickness or higher phosphor concentration for Method V in the variation ranges, the brightness difference can be further reduced according to (6) and can be comparable with that other methods. As a result, Method V can fulfill the requirements of both high color consistency and high brightness consistency.

IV. Conclusion

Conformal phosphor coating is widely adopted in current LED packaging. The color consistency of this method is acceptable but its brightness consistency is poor. The brightness level of this method is low and shifts greatly, showing a strong dependence on the variations of the phosphor thickness and concentration. Recently proposed packaging method using planar remoter phosphor shows improvements of the brightness consistency and the brightness level. But the color consistency is deteriorated due to the smaller variation ranges of the phosphor thickness and the concentration. Reducing the distance of the remote phosphor can further improve the brightness level and make the variation range of the luminous efficiency more stable. But this method also cannot avoid the issue of poor color consistency. Changing the planar remoter phosphor to be hemispherical remoter phosphor can fulfill the requirements of both high color consistency and high brightness consistency due to its capability of larger variation ranges of the phosphor thickness and the concentration in the same color binning. The brightness level of this method is also the highest and can be confined in small range, especially when applying thick phosphor thickness or high phosphor concentration. All of these significant improvements make the hemispherical remoter phosphor a promising choice for the low cost production of white LEDs.

Acknowledgment

The authors would like to thank the Science and Technology Department of Guangdong Province and Guangdong Real Faith Enterprises Group Co. Ltd. for their support.

References

[1] M. R. Krames, O. B. Shchekin, R. Mueller-Mach, G. O. Mueller, L. Zhou, G. Harbers, and M. G. Craford, "Status and future of high-power light-emitting diodes for solid-state lighting," *IEEE J. Display Technol.*, vol. 3, no. 2, pp. 160–175, Jun. 2007.

[2] R. D. Dupuis and M. R. Krames, "History, development, and applications of high-brightness visible light-emitting diodes," *IEEE J. Lightwave Technol.*, vol. 26, no. 9, pp. 1154–1171, May 2008.

[3] E. F. Schubert and J. K. Kim, "Solid-state light source getting smart," *Science*, vol. 308, no. 27, pp. 1274–1278, May 2005.

[4] S. Nakamura, S. Pearton, and G. Fasol, *The Blue Laser Diode: GaN based light emitters and lasers*, 2nd ed. Berlin, Germany: Springer, 1997, pp. 230–234.

[5] F. M. Steranka, J. C. Bhat, D. Collins, L. Cook, M. G. Craford, R. Fletcher, N. Gardner, P. Grillot, W. Goetz, M. Keuper, R. Khare, A. Kim, M. Krames, G. Harbers, M. Ludowise, P. S. Martin, M. Misra, G. Mueller, R. Mueller-Mach, S. Rudaz, Y. C. Shen, D. Steigerwald, S. Stockman, S. Subramanya, T. Trottier, and J. J. Wierer, "High power LEDs-technology status and market applications," *Physica Status Solidi (a)*, vol. 194, no. 2, pp. 380–388, Dec. 2002.

[6] K. Wang, X. B. Luo, Z. Y. Liu, B. Zhou, Z. Y. Gan, and S. Liu, "Optical analysis of an 80-W light-emitting-diode street lamp," *Optic. Eng.*, vol. 47, no. 1, pp. 013002-1–013002-13, 2008.

[7] J. K. Kim and E. F. Schubert, "Transcending the replacement paradigm of solid-state lighting," *Opt. Express*, vol. 16, no. 26, pp. 21835–21842, 2008.

[8] Z. Liu, S. Liu, K. Wang, and X. Luo, "Status and prospect for phosphor-based white light-emitting diodes packaging," *Frontiers Optoelectron. China*, vol. 2, no. 2, pp. 119–140, 2009.

[9] G. H. Negley and M. Leung, "Methods of coating semiconductor light emitting elements by evaporation solvent from a suspension (Patent style)," U.S. Patent 20 070 224 716, May 1, 2007.

[10] W. D. Collins, M. R. Krames, G. J. Verhoeckx, and N. J. M. Leth, "Using electrophoresis to produce a conformal coated phosphor-converted light emitting semiconductor (Patent style)," U.S. Patent 6 576 488, Jun. 11, 2001.

[11] H. Bechtel, P. Schmidt, W. Busselt, and B. S. Schreinemacher, "Lumiramic: A new phosphor technology for high performance solid state light sources," in *Proc. 8th Int. Conf. Solid State Lighting*, 2008, pp. 70580E-1–70580E-10.

[12] B. Braune, K. Petersen, J. Strauss, P. Kromotis, and M. Kaempf, "A new wafer level coating technique to reduce the color distribution of LEDs," in *Proc. Light-Emitting Diodes: Research, Manufacturing, Applications XI*, 2007, pp. 64860X-1–64860X-11.

[13] H. Luo, J. K. Kim, E. F. Schubert, J. Cho, C. Sone, and Y. Park, "Analysis of high-power packages for phosphor-based white-light-emitting diodes," *Appl. Phys. Lett.*, vol. 86, p. 243505, Jun. 2005.
[14] J. K. Kim, H. Luo, E. F. Schubert, J. Cho, C. Sone, and Y. Park, "Strongly enhanced phosphor efficiency in GaInN white light-emitting diodes using remote phosphor configuration and diffuse reflector cup," *Japanese J. Appl. Phys.*, vol. 44, no. 21, pp. L649–L651, 2005.
[15] N. Narendran, "Improved performance white LED," in *Proc. 5th Int. Conf. Solid State Lighting*, 2005, pp. 594108-1–594108-6.
[16] N. Narendran, F. Gu, J. P. Freyssinier-Nova, and Y. Zhu, "Extracting phosphor-scattered photons to improve white LED efficiency," *Physica Status Solidi (a)*, vol. 202, no. 6, pp. R60–R62, 2005.
[17] G. Muller, R. Muller, G. Basin, R. S. West, P. S. Martin, T. S. Lim, and S. Eberle, "LED with phosphor tile and overmolded phosphor in lens (Patent style)," U.S. Patent 20 080 048 200, Feb. 26, 2008.
[18] Z. Y. Liu, S. Liu, K. Wang, and X. B. Luo, "Optical analysis of phosphor's location for high-power light-emitting diodes," *IEEE Trans. Device Materials Rel.*, vol. 9, no. 1, pp. 65–73, Mar. 2009.
[19] C. Sommer, F. P. Wenzl, P. Hartmann, P. Pachler, M. Schweighart, and G. Leising, "Tailoring of the color conversion elements in phosphor-converted high-power LEDs by optical simulations," *IEEE Photonics Technol. Lett.*, vol. 20, no. 5, pp. 739–741, Mar. 2008.
[20] E. F. Schubert, *Light-Emitting Diodes*. New York: Cambridge Univ. Press, 2006, pp. 163–189.
[21] T.-X. Lee, K.-F. Gao, W.-T. Chien, and C.-C. Sun, "Light extraction analysis of GaN-based light-emitting diodes with surface texture and/or patterned substrate," *Optics Express*, vol. 15, no. 11, pp. 6670–6676, May 2007.
[22] A. Zukauskas, M. S. Shur, and R. Gaska, *Introduction to Solid-State Lighting*. New York: John Wiley, 2002, pp. 95–99.
[23] W. Heller, "Remarks on refractive index mixture rules," *J. Physical Chemistry*, vol. 69, no. 4, pp. 1123–1129, 1965.
[24] M. I. Mishchenko, L. D. Travis, and A. A. Lacis, *Scattering, Absorption, and Emission of Light by Small Particles*. Cambridge, U.K.: Cambridge University Press, 2004, pp. 31–60.
[25] D.-Y. Kang, E. Wu, and D.-M. Wang, "Modeling white light-emitting diodes with phosphor layers," *Appl. Phys. Lett.*, vol. 89, no. 23, p. 231102, 2006.
[26] Y. Zhu, N. Narendran, and Y. Gu, "Investigation of the optical properties of YAG:Ce phosphor," in *Proc. 6th Int. Conf. Solid State Lighting*, 2006, pp. 63370S-1–63370S-8.
[27] S. C. Allen and A. J. Steckl, "ELiXIR-solid-state luminaire with enhanced light extraction by internal reflection," *J. Display Technol.*, vol. 3, no. 2, pp. 155–159, 2007.
[28] R. Mueller-Mach, G. O. Mueller, and M. R. Krames, "Phosphor materials and combinations for illumination-grade white PCLEDs," in *Proc. 3rd Int. Conf. Solid State Lighting*, 2004, pp. 115–122.
[29] M. Zachau, D. Becker, D. Berben, T. Fiedler, F. Jermann, and F. Zwaschka, "Phosphors for solid state lighting," in *Proc. Light-Emitting Diodes: Res., Manuf., Appl. XII*, 2008, p. 691010.
[30] W. Falicoff, J. Chaves, and B. Parkyn, "PC-LED luminance enhancement due to phosphor scattering," in *Proc. Nonimaging Optics Efficient Illumination Syst. II*, 2005, pp. 59420N-1–59420N-15.
[31] A. Borbely and S. G. Johnson, "Performance of phosphor-coated LED optics in ray trace simulations," in *Proc. 4th Int. Conf. Solid State Lighting*, 2004, pp. 266–273.
[32] N. T. Tran and F. G. Shi, "Studies of phosphor concentration and thickness for phosphor-based white light-emitting diodes," *J. Lightwave Technol.*, vol. 26, no. 21, pp. 3556–3559, 2008.

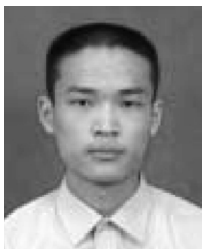

Zongyuan Liu received the B.E. degree in mechanical science design and manufacturing and automation in 2006 from the School of Mechanical Science and Engineering, Huazhong University of Science and Technology, Wuhan, China, where he has been working toward the Ph.D. degree in precision manufacturing engineering. He is also with the Wuhan National Laboratory for Optoelectronics, Wuhan, as a Ph.D. candidate.

His current research interests include high-power-LED packaging, rheology of silicones and LEDs lamp design.

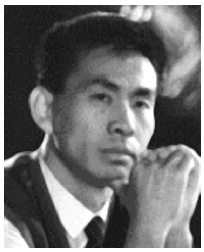

Sheng Liu (SM'09) received the B.S. and M.S. degrees in flight vehicle design from the Nanjing Univeristy of Aeronautics and Astronautics, Nanjing, China, in 1983, and 1986, respectively, and the Ph.D. degree in mechanical engineering from Stanford University, Stanford, CA, in 1992.

He has over 14 years experience in integrated circuit (IC) packaging, 8 years in micro-electro-mechanical systems (MEMS) packaging, and 4 years in optoelectronic/LED packaging. From 1992 to 1995, he was an Assistant Professor with the School of Mechanical and Aerospace Engineering, Florida Institute of Technology, Melbourne, FL. In 1995, he became an Assistant Professor with the School of Mechanical Engineering and the Institute for Manufacturing Research (Joint Appointment), Wayne State University, Detroit, MI, where he became an Associate Professor in 1998. In 2004, he came back to Huazhong University of Science and Technology, Wuhan, China, where he became a specially recruited Full Professor with the School of Mechanical Science and Engineering, and the Director of the Institute of Microsystems. He is currently the Director with the Division of Micro-Opto-Electronic-Mechanical Systems, Wuhan National Laboratory for Optoelectronics, Wuhan. His current research interests include LED/MEMS/IC packaging, mechanics, and sensors.

Kai Wang received the B.S. degree in optical information science and technology in 2006 from the Huazhong University of Science and Technology, Wuhan, China, where he spent one year studying for his Master's degree. He has been pursuing the Ph.D. degree in optoelectronics information engineering since 2007. He is currently a Ph.D. candidate with the Wuhan National Laboratory for Optoelectronics, Wuhan.

His current research interests include the optical design of light-emitting diode packaging and application.

Xiaobing Luo (M'07) received the B.E. degree in thermal energy and powering engineering in 1995 and the M.E. degree in engineering thermophysics in 1998 from Huazhong University of Science and Technology, Wuhan, China, and the Ph.D. degree in engineering thermophysics in 2002 from Tsinghua University, Beijing, China.

From 2002 to 2005, he was with Samsung Electronics, Seoul, Korea, as a Senior Engineer. In 2005, he became an Associate Professor with the School of Energy and Power Engineering, Huazhong University of Science and Technology, Wuhan, and in 2007, he became a Full Professor. He is also a Professor with the Wuhan National Laboratory for Optoelectronics, Wuhan. His current research interests include light-emitting diode, heat and mass transfer, microfluidics, microelectro-mechanical systems, sensors and actuators.